Differential tumor-targeting abilities of three single-domain antibody formats

Bell, Andrea; Wang, Zheng J.; Arbabi-Ghahroudi, Mehdi; Chang, Tingtung A.; Durocher, Yves; Trojahn, Ulrike; Baardsnes, Jason; Jaramillo, Maria L.; Li, Shenghua; Baral, Toya N.; O'Connor-McCourt, Maureen; MacKenzie, Roger; Zhang, Jianbing

Publisher's version / Version de l'éditeur:
http://dx.doi.org/10.1016/j.canlet.2009.08.003
Cancer Letters, 289, 1, pp. 81-90, 2010-03-01

Cancer Letters 289 (2010) 81–90

Contents lists available at ScienceDirect

Cancer Letters

journal homepage: www.elsevier.com/locate/canlet

Differential tumor-targeting abilities of three single-domain antibody formats

Andrea Bell [a], Zheng J. Wang [b], Mehdi Arbabi-Ghahroudi [a], Tingtung A. Chang [b], Yves Durocher [c], Ulrike Trojahn [c], Jason Baardsnes [c], Maria L. Jaramillo [c], Shenghua Li [a], Toya N. Baral [a], Maureen O'Connor-McCourt [c], Roger MacKenzie [a], Jianbing Zhang [a,*]

[a] Institute for Biological Sciences, National Research Council of Canada, 100 Sussex Drive, Ottawa, ON, Canada K1A 0R6
[b] Department of Radiology, The University of Texas HSC at San Antonio, 7703 Floyd Curl Drive, San Antonio, TX 78229-3900, USA
[c] Biotechnology Research Institute, National Research Council of Canada, 6100 Royalmount Avenue, Montreal, QC, Canada H4P 2R2

ARTICLE INFO

Article history:
Received 26 March 2009
Received in revised form 22 July 2009
Accepted 2 August 2009

Keywords:
Epidermal growth factor receptor
(Chimeric) heavy chain antibody
Single-domain antibody

ABSTRACT

The large molecular size of antibody drugs is considered one major factor preventing them from becoming more efficient therapeutics. Variable regions of heavy chain antibodies (HCAbs), or single-domain antibodies (sdAbs), are ideal building blocks for smaller antibodies due to their molecular size and enhanced stability. In the search for better antibody formats for *in vivo* imaging and/or therapy of cancer, three types of sdAb-based molecules directed against epidermal growth factor receptor (EGFR) were constructed, characterized and tested. Eleven sdAbs were isolated from a phage display library constructed from the sdAb repertoire of a llama immunized with a variant of EGFR. A pentameric sdAb, or pentabody, V2C-EG2 was constructed by fusing one of the sdAbs, EG2, to a pentamerization protein domain. A chimeric HCAb (cHCAb), EG2-hFc, was constructed by fusing EG2 to the fragment crystallizable (Fc) of human IgG1. Whereas EG2 and V2C-EG2 localized mainly in the kidneys after *i.v.* injection, EG2-hFc exhibited excellent tumor accumulation, and this was largely attributed to its long serum half life, which is comparable to that of IgGs. The moderate size (~80 kDa) and intact human Fc make HCAbs a unique antibody format which may outperform whole IgGs as imaging and therapeutic reagents.

1. Introduction

Epidermal growth factor receptors (EGFRs) are overexpressed and/or dysregulated in many tumor types including head and neck, breast, non-small-cell lung and pancreatic cancer to name but a few [1]. The EGFR family contains four members: EGFR1 (ErbB1), HER2 (ErbB2), HER3 (ErbB3) and HER4 (ErbB4) [2]. Targeting EGFR in cancer cells was initially proposed by Sato et al. [3]. The anti-EGFR antibody drug Cetuximab (Erbitux^{R}) was approved by the FDA in 2004 for the treatment of metastatic colon cancer either in combination with Camptosar, a chemotherapeutic, or as a single agent for patients who cannot tolerate chemotherapy.

Despite the success of Cetuximab and other antibody drugs, their large size (~150 kDa) is considered a major limiting factor in tumor penetration [4] and in achieving a higher therapeutic index. To generate antibodies with improved tumor penetration, many antibody formats have been engineered and tested. Single chain variable fragments (scFvs) are often cleared rapidly from circulation partly due to their low molecular weight (MW < 60 kDa, the threshold of glomerular filtration) [5]. As a result, scFvs usually have a serum half life of less than 10 min and a peak tumor uptake of about 5% injected dose per gram tissue (% ID/g) [4]. The performance of scFvs can be improved by constructing divalent scFvs [6], tetravalent scFvs [6] and

* Corresponding author. Tel.: +1 613 998 3373; fax: +1 613 952 9092.
E-mail address: Jianbing.zhang@nrc.ca (J. Zhang).

0304-3835/$ - see front matter Crown Copyright © 2009 Published by Elsevier Ireland Ltd. All rights reserved.
doi:10.1016/j.canlet.2009.08.003

minibodies [7]. However, the overall performance of these molecules is still less than optimal. In addition, most smaller size antibody fragments lack intact fragment crystallizable (Fc) domain and are therefore unable to induce antibody-dependent cellular cytotoxicity (ADCC) and complement-dependent cytotoxicity (CDC), two major mechanisms involved in the eradication of tumor tissue upon antigen binding [8].

By fusing a scFv to the Fc domain, a novel antibody molecule scFv-Fc, which self assembled into a dimer with a molecular weight of about 105 kDa [9], was generated. This antibody format, when incorporating Fc mutants with different affinities for neonatal Fc receptor (FcRn), generated excellent tumor-targeting antibodies with tumor uptake as high as 44% ID/g [10]. This makes scFv-Fc a potentially better antibody platform for early tumor detection, radioimmunotherapy and therapy than intact IgG. However, it is almost impossible to further reduce antibody size when combining an intact Fc with scFvs.

Single-domain antibodies (sdAbs), often referred to as domain antibodies (dAbs) when based on either heavy chain or light chain variable regions of human antibodies [11,12] or nanobodies when derived from the variable regions of HCAbs of camelids [13], are the smallest antigen binding fragments with a size of 12–15 kDa. Single-domain antibodies can also be derived from the new antigen receptor antibodies (IgNARs) of nurse sharks [14]. Camelids such as camels, llamas and alpacas have HCAbs naturally devoid of light chains and consist only of V_H, C_H2 and C_H3 domains [13]. sdAbs derived from camelid HCAbs are excellent building blocks for novel antibody molecules [15] due to their high thermostability, high detergent resistance, relatively high resistanceto proteases [16] and high production yield [17]. They can be engineered to have very high affinity by isolation from an immune library [18] or by *in vitro* affinity maturation [19,20].

Despite the immense potential of sdAbs, tumor-targeting with sdAbs remains largely unexplored. Monomeric (15 kDa) and bivalent (33 kDa) sdAbs targeting lysozyme, which was expressed as an artificial target on the surface of a tumor cell line, were isolated, constructed and tested [21]. However, these molecules failed to show sufficient tumor accumulation due largely to rapid blood clearance. Anti-CEA sdAbs were isolated and fused to the β-lactamase of *Enterobacter cloacae*. The fusion protein was shown to efficiently activate prodrug in an *in vitro* study and induce tumor regression in an established tumor xenograft model [22]. A similar approach was used to link a sdAb against Type IV collagenase with an anti-tumor drug, lidamycin, and the fusion protein also demonstrated tumor growth inhibition [23]. sdAbs against EGFR [24] and its Type III variant [25] have been isolated. Some of these sdAbs were found to be useful for tumor imaging despite of their high renal uptake [26,27]. Although these studies demonstrate the potential uses of sdAbs, establishment of a versatile sdAb-based antibody platform, especially one that improves circulating half life, would further stimulate development of sdAb-based drugs.

We describe in this study the isolation of EGFR-specific sdAbs and engineering of three types of sdAb-based molecules: sdAb (one antigen binding site, ~16 kDa), pentabody (five antigen binding sites, ~126 kDa) and chimeric HCAb (cHCAb) (two antigen binding sites, ~80 kDa without consideration of glycosylation). We also present an evaluation of the tumor-targeting ability of the molecules using micro-positron emission tomography (microPET).

2. Materials and methods

2.1. Cells and animals

The human pancreatic carcinoma cell line MIA PaCa-2 was kindly provided by Dr. I. Kazhdan and maintained in DMEM (Gibco, Gaithersburg, MD) supplemented with 10% fetal bovine serum (Gibco). Six-week old female BALB/c nude mice were obtained from Harlan Laboratories.

2.2. Construction and purification of the extracellular domains of EGFR and EGFRvIII

Sub-cloning, production and purification of the extracellular domains of EGFR (EGFR-ECD) was performed as previously described [28]. Recombinant baculoviruses containing the coding sequences for 6× Histidine (His)-tagged extracellular domains EGFR and EGFRvIII [29] were used to infect Sf9 (Invitrogen, Burlington, ON) cells growing in suspension at 5–10 × 10^6 cells/ml. Purification of the secreted proteins was performed by immobilized metal affinity chromatography (IMAC) using Ni-NTA-agarose (Qiagen, Mississauga, ON) following the manufacturer's instructions. Purified EGFR-ECD and EGFRvIII-ECD were confirmed by SDS–PAGE.

2.3. Isolation of EGFR-specific sdAbs from a llama immune phage display library

A male llama (*Lama glama*) was injected subcutaneously with 100, 75, 75, 50 and 50 μg EGFRvIII-ECD on days 1, 21, 36, 50 and 64, respectively [17]. Complete Freund's Adjuvant (Sigma, St. Louis, MO) was used for the primary immunization and Incomplete Freund's Adjuvant was used for immunizations 2–4. Adjuvant was not used for the final immunization. The llama was bled one week following each immunization and heparinized blood was collected for immediate isolation of the peripheral blood leukocytes, which were then stored at −80 °C until further use.

Total RNA was isolated from 2 × 10^7 leukocytes using a QIAamp RNA Blood Mini Kit (Qiagen). cDNA was synthesized using $pd(N)_6$ as primer and 566 ng total RNA as the template. Three different sense primers (called J′ and corresponding to the 5′-end of IgG) including MJ1 (GCCCAGCCGGCCATGGCCSMKGTGCAGCTGGTGGAKTCTG-GGGGA), MJ2 (CAGCCGGCCATGGCCCAGGTAAAGCTGGAGGAGTCTG-GGGGA) and MJ3 (GCCCAGCCGGCCATGGCCCAGGCTCAGG-TACAGCTGGTGGAGTCT) and two anti-sense primers, corresponding to the C_H2 domain DNA sequence, C_H2 (CGCCATCAAGGTACCAGTTGA) and C_H2_b3 (GGGGTACCTGT-CATCCACGGACCAGCTGA) were used to amplify the V_H-C_H1-Hinge-C_H2 region of conventional IgG or V_HH-Hinge-C_H2. Amplified V_HH products of approximately 600 bp from the primer combination J′-C_H2 were extracted from a 1%

agarose gel and purified with a QIAquick Gel Extraction Kit (Qiagen) and the amplified products from primers J′-C_H2_b3 were PCR purified. In a second PCR reaction, two primers, MJ7BACK (CATGTGTAGACTCGCGGCCCAGCCGGCCATGGCC) and MJ8FOR (CATGTGTAGATTCCTGGCCGGCCTGGCCTGAGGAGACGGTGACCTGG), were used to introduce *Sfi*I restriction sites and to amplify the final sdAb fragments from the combined J′-C_H2 and J′-C_H2_b3 amplified products [17]. The final PCR product was digested with *Sfi*I and ligated into pMED1, a derivative of pHEN4 [17], and transformed into *Escherichia coli* TG1 (New England Biolabs, Ipswich, MA) by electroporation. Phage were rescued and amplified with helper phage M13KO7 (NEB).

The llama immune phage display library was panned against 1 mg/ml EGFRvIII-ECD that was coated to a Reacti-Bind™ maleic anhydride activated microtiter plate well. Approximately 10^{11} phages were added to the well and incubated at 37 °C for 2 h for antigen binding. After disposal of unbound phages, the wells were washed six times with phosphate buffered saline supplemented with 0.05% Tween 20 (PBST) for round one and the washes were increased by one for each additional round. Phage were eluted by 10 min incubation with 100 μl 100 mM triethylamine and the eluate was subsequently neutralized with 200 μl 1 M Tris–HCl (pH 7.5). Phage were amplified as described above but on a smaller scale. After four rounds of panning, eluted phage were used to infect exponentially growing *E. coli* TG1. Individual colonies were used in phage ELISA.

For phage ELISA, a 96-well microtitre plate was coated overnight with 5 μg/ml EGFRvIII-ECD or EGFR-ECD and then blocked with 1% casein for 2 h at 37 °C. Phage from individual clones were pre-blocked with 1% casein overnight, added to the pre-blocked wells and incubated for 1 h. Phage ELISA was performed using the GE Healthcare Detection Module Recombinant Phage Antibody System (GE Healthcare, Uppsala, Sweden), and positive phage clones were sequenced.

2.4. Expression of sdAbs and a pentabody

DNA encoding four representative clones (EG2, EG10, EG31 and EG43) from each of the four groups (Fig. 1) was cloned into the *Bbs*I and *Bam*HI sites of a periplasmic expression vector pSJF2 [30], which added a c-Myc detection tag and a 5× His purification tag at the C-terminus of the sdAbs (Fig. 2A). EG2 was sub-cloned into the *Bsp*EI and *Bam*HI sites of a pentamerization vector, pVT2 [31], generating an expression vector for pentameric sdAb, or pentabody, V2C-EG2 (Fig. 2A). EG2 and pV2C-EG2 were expressed periplasmically and purified by IMAC [32]. Briefly, clones were inoculated in 25 ml LB-Ampicillin (Amp) and incubated at 37 °C with 200 rpm shaking overnight. The next day, 20 ml of the culture was used to inoculate 1 l of M9 medium (0.2% glucose, 0.6% Na_2HPO_4, 0.3% KH_2PO_4, 0.1% NH_4Cl, 0.05% NaCl, 1 mM $MgCl_2$, 0.1 mM $CaCl_2$) supplemented with 0.4% casamino acids, 5 mg/l of vitamin B1 and 200 μg/ml of Amp, and cultured for 24 h. 100 ml of 10 × TB nutrients (12% Tryptone, 24% yeast extract and 4% glycerol), 2 ml of 100 mg/ml Amp and 1 ml of 1 M isopropyl-beta-D-Thiogalactopyranoside (IPTG) were added to the culture and incubation was continued for another 65–70 h at 28 °C with 200 rpm shaking. *E. coli* cells were harvested by centrifugation and lysed with lysozyme. Cell

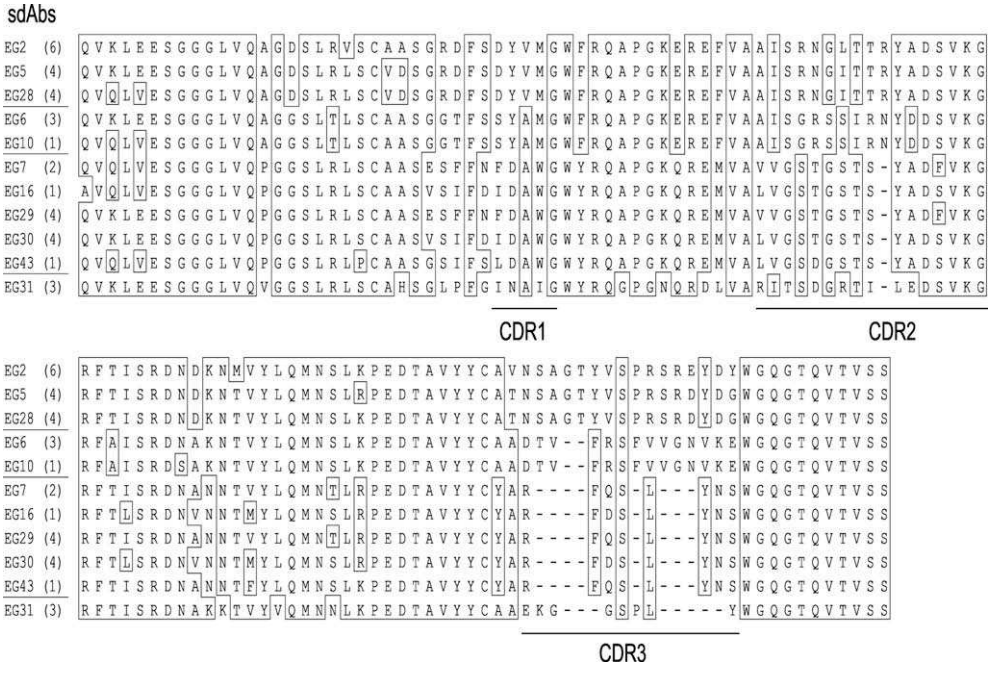

Fig. 1. Amino acid sequences of 11 sdAbs specific for EGFR with CDR1, CDR2, and CDR3 underlined. Based on the sequence identity of their CDRs, the sdAbs can be divided into four groups, which are separated by horizontal lines between the clone designations. The frequency of the sequences is indicated in parentheses following the clone designations.

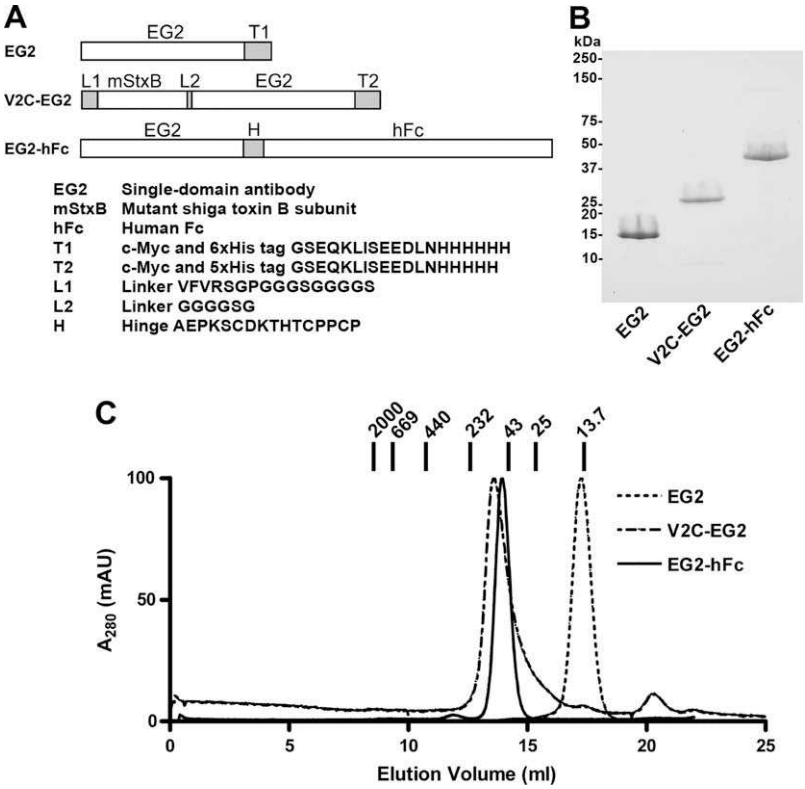

Fig. 2. Antibody molecules constructed in this study. (A) Schematic representation of the primary structures of the sdAb (EG2), the pentabody (V2C-EG2) and the cHCAb (EG2-hFc). (B) SDS–PAGE of 1 μg purified EG2, V2C-EG2, and EG2-hFc. EG2 and V2C-EG2 were expressed in *E. coli*, and EG2-hFc was expressed in HEK293 cells. Proteins were separated on an 8–25% gradient PhastGel and Coomassie stained to visualize the proteins. (C) Size exclusion chromatography of purified EG2, V2C-EG2, and EG2-hFc using a Superdex 200™ column. Superdex separations were carried out in PBS. The elution positions of molecular mass markers are indicated. Data are normalized to a maximum 100 milliabsorbance units.

lysates were centrifuged, and clear supernatant was loaded onto High-Trap™ chelating affinity columns (GE Healthcare) and His-tagged proteins were purified.

2.5. Construction of cHCAb EG2-hFc

Human Fc (hFc) gene, a gift from Dr. M. Neuberger, was inserted into a mammalian expression vector pTT5, a derivative of the pTT vector [33], to generate hFc fusion vector pTT5-hFc [34]. EG2 was amplified and inserted into pTT5-hFc such that the C-terminus of the sdAb was linked to the hinge region and Fc of human IgG1 without addition of extra residues. The generated EG2-hFc was used in the transient transfection of HEK293 cells.

Clone 6E of 293-EBNA1 (Y.D., unpublished data) was maintained as a suspension culture in shake flasks in serum-free F17 medium (Invitrogen, Burlington, ON). Cells were inoculated at a density of 0.25×10^6 cells/ml in a 2.5 l shake flask (500 ml working volume) two days prior to transfection. Cells (usually around $1.0–1.5 \times 10^6$ cells/ml) were transfected with 1 μg/ml plasmid DNA and 2 μg/ml linear 25 kDa polyethyleneimine, as previously described [33]. A feed with TN1 peptone (0.5%) was performed 24 h post-transfection [35] and culture medium was harvested at 120 h. EG2-hFc secreted into the medium was purified by affinity chromatography on a Protein A column, MabSelect SuRe (GE Healthcare). Purified material was desalted on a HiPrep™ 26/10 desalting column (GE Healthcare) equilibrated with phosphate buffered saline (PBS). Protein concentration was determined by absorbance at 280 nm using a molar extinction coefficient of 58,830 calculated from the EG2-hFc amino acid sequence [36].

2.6. Surface plasmon resonance analysis

Experiments were performed using a BIACORE 3000 optical sensor platform and research grade CM5 sensor chips (GE Healthcare). EGFR-ECD, sdAbs or multivalent sdAb constructs were immobilized on the sensor chip surface by standard amine coupling. All experiments were carried out in HEPES buffer (10 mM HEPES (pH 7.4), 150 mM NaCl, 3.4 mM EDTA, 0.005% Tween 20) at 25 °C. Antibodies were injected at serial dilutions ranging from 0.4 nM to 1 μM at a flow rate of 30 μl/min unless otherwise indicated. The amount of bound analyte after subtraction from the blank control surface is shown as relative resonance units (RU). The double referenced sensorgrams from each injection series were analyzed for binding kinetics using BIAevaluation software (GE Healthcare). Dissociation constants (K_Ds) were calculated from the on- and off-rates (k_{on} and k_{off}, respectively), as determined by global fitting

of the experimental data to a 1:1 Langmuir binding model ($Chi^2 < 1$).

2.7. Size exclusion chromatography

Size exclusion chromatography (SEC) of EG2, V2C-EG2 and EG2-hFc was performed on Superdex 200™ (GE Healthcare). Superdex separations were carried out in PBS. Low MW markers ribonuclease A (13.7 kDa), chymotrypsin A (25 kDa) and ovalbumin (43 kDa) were used to calculate the MW of EG2. High MW markers catalase (232 kDa), ferritin (440 kDa), thyroglobulin (669 kDa) and blue dextran (2000 kDa) were used to calculate the MW of V2C-EG2 and EG2-hFc.

2.8. ^{64}Cu-labeling of antibodies

1,4,7,10-Tetraazacyclododecane-N,N′,N″,N‴-tetraacetic acid (DOTA) was activated by N-hydroxysulfosuccinimide (sulfo-NHS) and 1-ethyl-3-[3-(dimethylamino)propyl] carbodiimide (EDC) in a mixture solution (pH 5.5) at 4 °C for 30 min. Purified antibody was reacted with a 1000:1000:100:1 M ratio of DOTA:sulfo-NHS:EDC:antibody in 0.1 M Na_2HPO_4 (pH 7.5) at 4 °C for 12–16 h. After conjugation, the reaction mixture was centrifuged repeatedly through a YM-30 centricon with 30 mM ammonium citrate buffer (pH 6.5) to remove unconjugated small molecules. The purified conjugate was concentrated to 1 mg/ml in 30 mM ammonium citrate buffer and stored at −20 °C for further use. Typically, 150 μg of DOTA-conjugated antibody and 3.70×10^7 Bq of ^{64}Cu ($^{64}CuCl_2$ in 0.1 M HCl; radionuclide purity >99%, Washington University, St. Louis, MO) were incubated in 30 mM ammonium citrate (pH 6.5) at 43 °C for 45 min. The reaction was terminated by addition of 5 μl 10 mM diethylenetriaminepentaacetic acid solution. Labeled antibody was separated by a size exclusion Bio-Spin™ 6 column (Bio-Rad, Mississauga, ON).

2.9. Micro-positron emission tomography/computed tomography (MicroPET/CT)

MIA PaCa-2 pancreatic cancer cells in 3×10^6 in sterile saline were injected subcutaneously into the right flank of the animals. The animal models were imaged when tumors reached the size of 300–500 mm^3. About 1.35×10^8 bq/120 μg of ^{64}Cu-DOTA-antibody was administered *via* tail vain injection to mice under Metofane anesthesia. The animals were allowed free access to food and water. The mice were re-anesthetized and imaged using microPET/CT scanner for 10 min at 1 and 4 h, 15 min at 20 h and 20 min at 44 h. MicroPET/CT imaging of mice was performed using a tri-modality microPET/CT/SPECT imager (Gamma Medica FLEX Inc., CA) for functional and anatomical imaging. MicroCT had an X-ray tube of 80 kVp, 0.5 mA fixed anode with tungsten target to provide anatomical imaging with spatial resolution of ~100 μm. Images were acquired at a fast scan time of 1 min and reconstructed using cone beam filtered back-projection (modified Feldkamp) reconstruction algorithm with streak artifact reduction. Live animal images were acquired at low radiation doses (1.2 cGy) for 1 min fly mode scan. Images were reconstructed using 2D filtered back-projection (2D OSEM) and 3D filtered back-projection (3D OSEM).

2.10. Quantification of microPET data

The calibration factor to convert PET image units of counts/sec/voxel to Bq/cc was calculated from a mouse-sized cylinder with a known concentration of ^{18}F in water assuming a tissue density of 1 g/cc. No additional attenuation correction was applied. The conversion of positron activity of ^{18}F to that of ^{64}Cu was carried out by the ratio of the branching ratios of the positron decay of the isotopes. The calculated concentrations of radioactivity were multiplied by the volume of each region of interest [37] to determine total radioactivity present within regions. ROI was analyzed using Analyzer AVW 3.0 software (Biomedical Imaging Resource, Mayo Foundation, Rochester, MN).

2.11. EG2-hFc blood clearance in mice

A group of five 6-week old female BALB/c nu/nu mice were *i.v.* injected with 150 μg EG2, V2C-EG2 or EG2-hFc in 100 μl PBS into the tail vein. Blood was collected from the facial vein at indicated time points. Sera were separated and stored at −20 °C until further use. Concentrations of the injected antibody molecules in the above collected samples were measured by ELISA. For ELISA, EGFR-ECD was coated on microtitre plates (Nunc) overnight at 4 °C at a concentration of 2 μg/ml. After washing three times with PBST, plates were blocked with 2% skimmed milk in PBS for one hour at 37 °C. Thousand times or ten thousand times diluted sera were added to the wells and incubated for another hour. Goat anti-llama antibody (1:1000) (Bethyl Lab, Montgomery, Maryland), HRP labeled anti-goat antibody (1:3000) (Cedarlane, Burlington, ON) and peroxidase substrate were used to detect EG2-based antibody molecules in the mouse sera. Serial dilutions of pure EG2-hFc in mouse serum were used to make a standard curve for EG2-hFc concentration analysis.

3. Results

3.1. Isolation and characterization of sdAbs

Isolation of EGFR-specific sdAbs was achieved by llama immunization with EGFRvIII-ECD, construction of an immune phage display library and subsequent panning. Llama leucocytes (2×10^7) were used for the isolation of mRNA, which was then used for the construction of a phage library with a size of 5.5×10^7. Four rounds of phage display panning were performed on immobilized EGFRvIII-ECD, and phage enrichment was observed during panning (data not shown). Phage ELISA showed that 44 of the 45 analyzed clones bound to EGFRvIII-ECD as well as wild type EGFR-ECD. Analysis of encoding sequences of the sdAbs displayed on the phage clones revealed 11 different sdAb genes. The Genebank Accession Numbers for the 11 sdAb genes are EG2, EU153238; EG5, EU153239; EG6, EU153240; EG7, EU153241; EG10, EU153242; EG16, EU153243; EG28, EU153244; EG29, EU153245; EG30, EU153246; EG31, EU153247, EG43, EU153248. The eleven sdAbs can be divided into four groups based on their CDR sequence identity (Fig. 1).

One sdAb gene from each of the four groups was chosen and subcloned into an *E. coli* periplasmic expression vector, pSJF2 [30], generating four clones pEG2, pEG10, pEG31 and pEG43. The four sdAbs, each tagged with a c-Myc detection tag and a 6× histidine (His) tag at their C-termini

(Fig. 2A, represented by EG2), were produced in *E. coli* and purified by IMAC. The yields of EG2, EG10, EG31 and EG43 were 11, 19, 8 and 43 mg per liter of TG1 culture, respectively.

The four anti-EGFR sdAbs were analyzed for binding to EGFR-ECD using a surface plasmon resonance (SPR)-based biosensor. The on-rates of the sdAbs range from 1×10^5 to 4×10^5 M^{-1} s^{-1} and the off-rates from 2.1×10^{-2} to 1.2×10^{-1} s^{-1}. The dissociation constants (K_Ds) of the sdAbs range from 55 nM (EG2) to 440 nM (EG31) (Fig. 3A, Table 1). EG2 was chosen for construction of two other antibody formats, pentabody and cHCAb, since this sdAb exhibited the highest affinity for EGFR.

Table 1
Kinetic rate constants and equilibrium rate constants of anti-EGFR sdAbs interacting EGFR-ECD.

sdAbs	EG2	EG10	EG31	EG43
k_{on} (M^{-1} s^{-1})	3.7×10^5	2.5×10^5	3.2×10^5	1.7×10^5
k_{off} (s^{-1})	2.1×10^{-2}	3.2×10^{-2}	1.4×10^{-1}	3.7×10^{-2}
K_D (nM)	55	126	440	316

3.2. Construction and characterization of EG2 pentabody and EG2 cHCAb

To construct EG2 pentabody, DNA encoding EG2 was amplified by PCR and flanked with restriction sites *Bsp*EI and *Bam*HI. The amplified DNA was digested and ligated into the pentamerization vector pVT2 [31] digested with the same enzymes. The generated clone expresses pentameric EG2, V2C-EG2 (Fig. 2A). The yield of V2C-EG2 was 44 mg per liter of *E. coli* culture.

To generate EG2 cHCAb, the sdAb gene was amplified and cloned into HCAb vector pTT5-hFc [34], which is designed to fuse a protein to the Fc domain of human IgG1. Sequence analysis of the generated clone, EG2-hFc, indicated that a Glu to Val mutation at position 5 of EG2 occurred during PCR amplification of EG2 but this did not affect the binding of EG2-hFc to EGFR (Fig. 3D). The generated construct (Fig. 2A) was used to transiently transfect human embryonic kidney cells HEK293. EG2-hFc was purified by Protein A affinity chromatography with a yield of 21 mg per liter of HEK293 culture.

EG2, V2C-EG2 and EG2-hFc were subjected to SDS–PAGE and size exclusion chromatography to analyze their subunit molecular weights and the molecular masses of the native proteins. Denatured EG2, V2C-EG2 and EG2-hFc migrated at 14 kDa, 23 kDa and 45 kDa, respectively (Fig. 2B). By size exclusion chromatography, the molecular masses of EG2, V2C-EG2 and EG2-hFc were estimated as 14, 108 and 90 kDa, respectively (Fig. 2C). These results demonstrate that EG2 exists as a monomer, V2C-EG2 as a pentamer and EG2-hFc as a dimer. The measured size of V2C-EG2 (108 kDa) is slightly smaller than the predicted size (126 kDa). Nevertheless, it is still considered a pentamer based on the electrophoretic and chromatographic data and the structure of the pentamerization domain, the B subunit of shiga toxin 1 (Stx1B) [38].

To evaluate the impact of multivalency on the functional affinities of V2C-EG2 and EG2-hFc, the binding profiles of these molecules were analyzed using the SPR-based biosensor by flowing them separately over the same EGFR-ECD surface. Oligomerization of EG2 sdAb, in either dimeric or pentameric format, resulted in higher apparent affinities (Fig. 3B and C). Although both proteins showed a slightly slower k_{on} compared to EG2 (data not shown), the main difference in apparent affinity is due to slower k_{off}s. This likely results from an avidity effect that occurs when a multivalent binder interacts with an immobilized protein. The avidity effect for the multivalent constructs, as reflected in a decrease in k_{off}, appears to increase with higher surface density of EGFR-ECD (comparing Fig. 3B

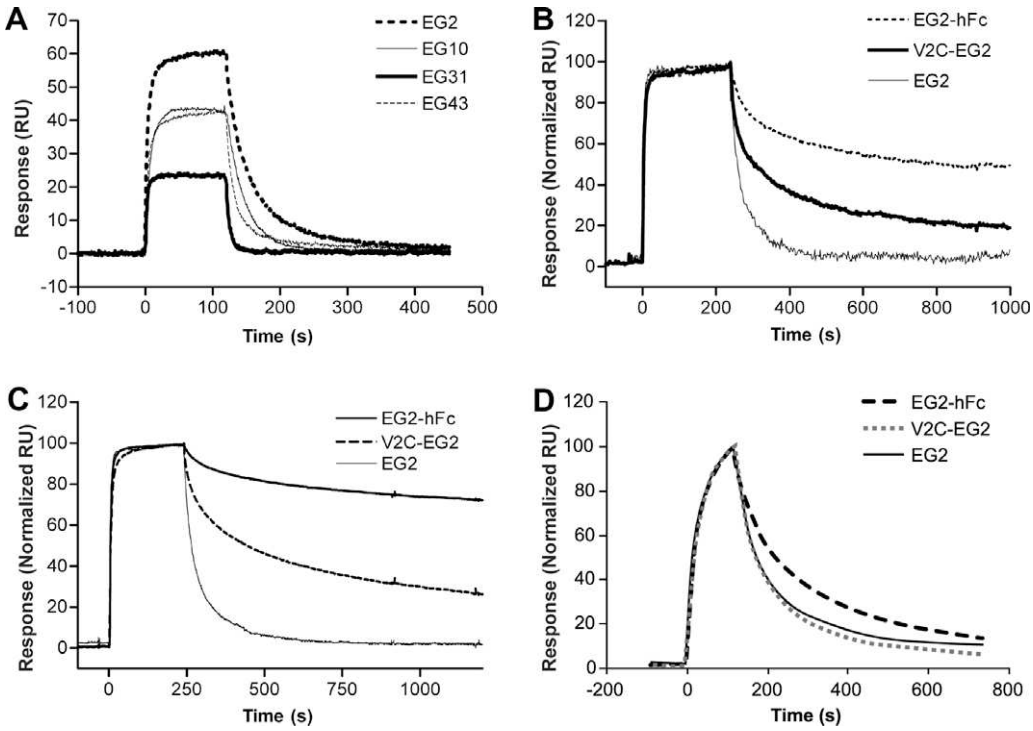

Fig. 3. Interactions between EGFR-ECD and various antibody constructs as monitored by surface plasmon resonance. (A) Sensorgrams showing 0.5 μM EG2, EG10, EG31, and EG43, injected at a flow rate of 20 μl/min, interacting with 500 RUs immobilized EGFR-ECD. For calculation of sdAb affinities, data from at least three independent experiments at sdAb concentrations ranging from 1 μM to 0.4 nM were fit to a 1:1 Langmuir binding model using BiaEvaluation v4.1. (B) and (C) Sensorgrams showing EG2, V2C-EG2, and EG2-hFc interacting with different antigen densities. EGFR-ECD was immobilized at a density of 400 RU (B) and 1500 RU (C) on the same sensor chip in different flow cells. EG2, V2C-EG2, and EG2-hFc interacting with antigen at different concentrations (1 μM to 0.4 nM) were analyzed; only the sensorgrams for the 0.5 μM injections are shown for clarity. The data in (B) and (C) were normalized to a maximum RU of 100 to allow better comparison of the dissociation phases between the antibody constructs. (D) Sensorgrams showing EGFR-ECD interacting with EG2, V2C-EG2, and EG2-hFc. The three antibodies were immobilized at a density of 300 RU. Concentrations of EGFR-ECD ranging from 1 μM to 0.4 nM were injected at a flow rate of 20 μl/min. The data at 0.5 μM were normalized to 100 RUs to show the near identity of the three interactions.

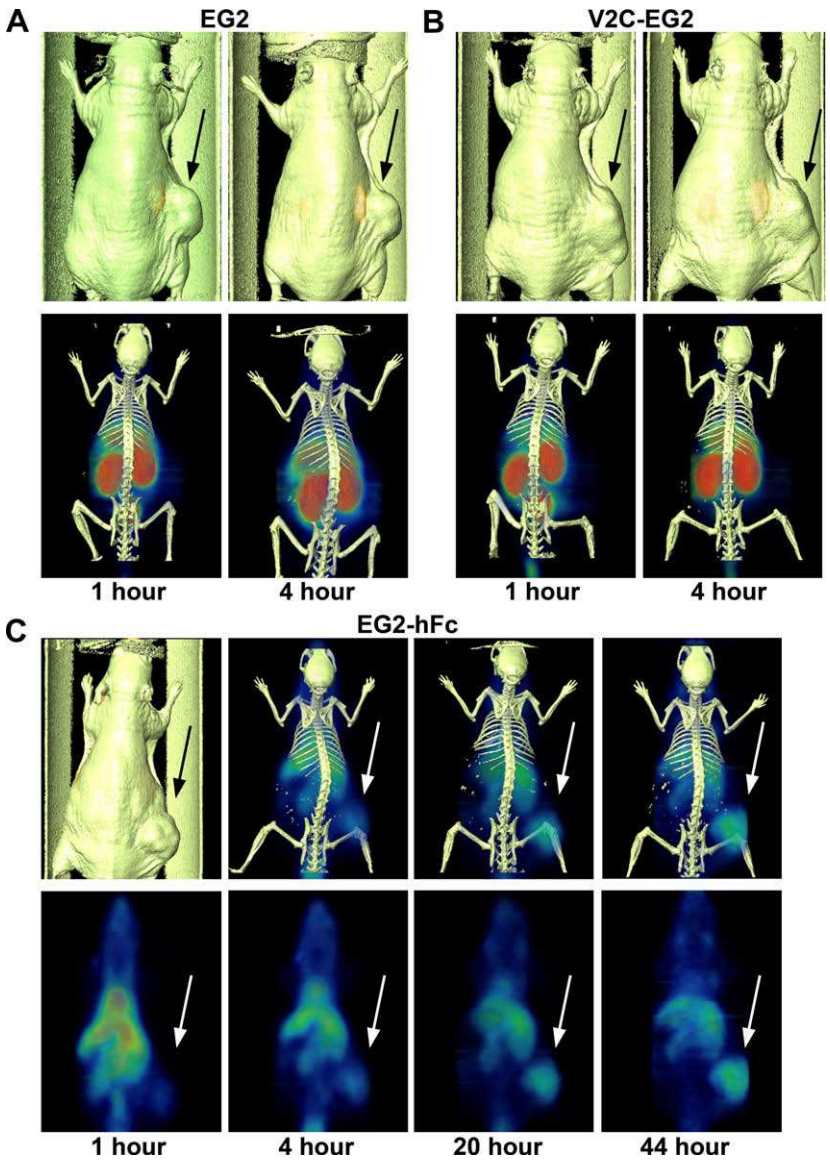

Fig. 4. Fused microPET/CT images of human pancreatic carcinoma model MIA PaCa-2. Mice bearing established tumors were *i.v.* injected with ^{64}Cu-DOTA-EG2 (A), ^{64}Cu-DOTA-V2C-EG2 (B), and ^{64}Cu-DOTA-EG2-hFc (C). For EG2 and V2C-EG2, the mice were imaged at 1 h, 4 h and 20 h post-injection (20 h data not shown). For EG2-hFc, the mouse was imaged at 1 h, 4 h, 20 h and 44 h post-injection. The top row in each sub-figure contains either surface rendering images performed using Amira™ (Mercury Computer System Inc.) to show relative tumor location (arrows) (Fig. 4A–C at 1 h) or fused microPET/CT images (Fig. 4C at 4, 20 and 44 h). The bottom row in each sub-figure contains either fused microPET/CT images (Fig. 4A and B) or microPET images (Fig. 4C). The images were acquired by FLEX Trimodality micro CT/PET/SPECT system (Gamma Medica-Ideas Inc.).

and C), as expected. In contrast, the K_D for EG2, the monomeric sdAb, was not affected by surface density. Although it is not possible to calculate accurate K_D values for V2C-EG2 and EG2-hFc due to their multivalency, fitting to 1:1 Langmuir binding model revealed an apparent K_D in the low nanomolar range (data not shown). It is expected that the pentavalent V2C-EG2 would have a slower dissociation rate than the bivalent EG2-hFc. However, the opposite was observed (Fig. 3B and C). A likely explanation is that not all five sdAbs are able to access immobilized antigen simultaneously.

To confirm that the higher apparent affinities of V2C-EG2 and EG2-hFc were indeed due to avidity effects resulting from multivalency, the experimental format was inversed such that EGFR-ECD binding to immobilized EG2, V2C-EG2 and EG2-hFc was analyzed by SPR. Sensorgrams of the interactions showed that EGFR-ECD binds to all three proteins, either monomer, dimer or pentamer, with nearly identical association and dissociation profiles (Fig. 3D). This result confirms that the improvements in apparent affinity of V2C-EG2 and EG2-hFc are due to their higher valency.

3.3. MicroPET/CT imaging of human pancreatic carcinoma model in nude mice

EG2, V2C-EG2 and EG2-hFc were labeled with ^{64}Cu and used for imaging a human pancreatic carcinoma model, MIA PaCa-2, established in one nude mouse for each construct. MicroPET/CT fused images suggested that the majority of EG2 and V2C-EG2 localized in the kidneys 1 h after injection (Fig. 4A and B). Both proteins were barely detectable in the tumor at

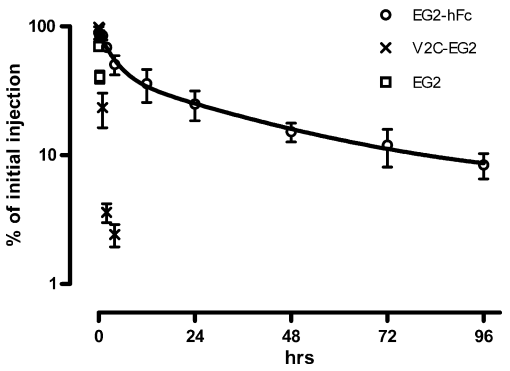

Fig. 5. Blood clearance profile of EG2, V2C-EG2, and EG2-hFc in BALB/c nu/nu mice. After *i.v.* injecting 150 μg different antibody constructs into the tail vein of the mice, concentrations of the molecules in the sera at indicated time points were measured by ELISA. EG2-hFc concentrations were fitted into a two-phase clearance model, as shown by the solid line.

1 h and 4 h. In contrast, microPET/CT images of the mouse administered with EG2-hFc revealed gradual accumulation in tumor and gradual reduction in other organs for the observed period (up to 44 h). No obvious kidney uptake was noticed (Fig. 4C). In addition, good tumor:muscle contrast was observed after 20 h, and the contour of the tumor in the PET image matches the true tumor shape.

3.4. Serum stability and serum clearance of the antibodies

The differential tumor-targeting ability of EG2, V2C-EG2 and EG2-hFc may relate to differences in stability in serum or serum half life of these molecules. sdAbs and pentabodies were found stable in serum [32]. To prove that EG2 and V2C-EG2 are stable as well and to evaluate the serum stability of EG2-hFc, all three proteins were incubated in serum for 24 h and assessed by ELISA after the incubation. All three proteins were found relatively stable in serum (data not shown).

An ELISA was then used to measure the concentrations of EG2, V2C-EG2 and EG2-hFc in mouse blood taken at different time points after injection. EG2 was cleared from the circulation relatively rapidly (Fig. 5). The circulating level of EG2 detected 1 h post-injection was only about 0.1% of the initial level observed at 0 h (this value is not visible due to the scales used in Fig. 5). This is in agreement with reports on other sdAbs [22]. V2C-EG2, despite its relatively large size of approximately 126 kDa, has only a slightly longer circulating half life (Fig. 5). Four hours after the injection, the amount of circulating V2C-EG2 was below the level of detection.

In contrast, EG2-hFc has a relatively long serum half life. The rate of removal of circulating EG2-hFc fits nicely into a two-phase clearance model (Fig. 5). The concentration of EG2-hFc 96 h post-injection was approximately 10% of its initial level. Comparing this result with that from a chimeric IgG targeting the same antigen in a similar animal models [39], it can be concluded that chimeric HCAb and chimeric IgG have similar serum half lives.

4. Discussion

The purpose of this study was to identify an appropriate sdAb-based antibody format which can be broadly used in targeting solid tumors as well as other disease states. We describe the isolation of eleven sdAbs targeting EGFR and the construction of pentabody (V2C-EG2) and cHCAb (EG2-hFc) versions of one of these sdAbs (EG2). These three versions of EG2 were radiolabeled with ^{64}Cu and microPET/CT imaging was used to analyze their *in vivo* distribution in a MIA PaCa-2 human pancreatic carcinoma xenograft model. As expected, the sdAb was cleared from the circulation rapidly after injection, and did not achieve significant tumor accumulation (Fig. 4A). The pentabody, despite its relatively large size (126 kDa), behaved similarly as the sdAb (Fig. 4B). Similar results were observed from other pentabodies used in tumor-targeting (J.Z. unpublished data), suggesting that pentabody is not an efficient tumor-targeting format. In contrast, the cHCAb achieved very good tumor accumulation over time. These results demonstrate that of the three formats, the cHCAb is by far the most suitable for tumor imaging and possibly cancer therapy. Similar results were obtained when the three formats were tested in a different EGFR-expressing tumor model and using a different contrast reagent (A. Abulrub, personal communication).

The tumor-targeting ability of an antibody is influenced predominantly by two rates: serum clearance rate and tumor penetration rate [40], which in turn are primarily influenced by affinity, size and the Fc region of the antibody. Intact Ig molecules are most frequently used in therapy due to their prolonged serum half lives. Truncated antibodies with a complete Fc domain, such as a scFv fused to C_H2–C_H3 (Fc), are cleared at a rate slightly faster than the original mAb [41,42]. By comparison, antibody fragments lacking the Fc domain, such as scFv and Fab, are rapidly cleared from the circulation by glomerular filtration, and have a much shorter serum half life [43].

Like scFvs, sdAbs including those reported by others [22] and described in this study also have short serum half lives, on the order of minutes. Our strategy of fusing sdAbs to either a pentamerization domain or an Fc domain was designed to increase not only the size of the sdAb to over 60 kDa, the glomerular filtration limit, but also its avidity. As expected, both pentamerized EG2 (V2C-EG2) and Fc-fused EG2 (EG2-hFc) exhibited avidity effects, albeit not to the same extent. It therefore follows that the slow blood clearance rate, rather than the avidity, of EG2-hFc is the characteristic that primarily accounts for its *in vivo* performance (Fig. 5).

Some data suggest that smaller antibody fragments penetrate into deeper areas of tumor tissue [44] but the loss of the Fc domain made them less attractive as imaging/therapeutic reagents. The challenge is to retain an intact Fc while satisfying the moderate size requirement for good tumor penetration. The small size (~14 kDa) of sdAbs makes it possible to fulfill both requirements. EG2-hFc, described here, has a complete human Fc domain and yet is only approximately 80 kDa. We refer to this type of molecule as a chimeric HCAb because it combines human Fc and camelid sdAb domains. Fully human HCAbs (hHCAbs) can be constructed if human sdAbs [11,45] are used. In addition, expression of cHCAbs in a mammalian expression system was tested by fusing six sdAbs to the Fc domain of human IgG1 with good yields [34]. Glycopatterns of these cHCAbs were found to be similar to human IgGs expressed in similar systems [34].

In summary, we propose that HCAbs warrant further investigation as alternatives to conventional IgGs for imaging and therapeutic applications because of (1) their potentially better tumor penetration; (2) their potentially higher production yield due to a simpler two-chain molecular structure; (3) their lower dose requirements due to lower molecular weight (~80 kDa *vs.* 150 kDa for IgG) and (4)

versatility, *i.e.* ease of construction of fusions to other effector entities.

Acknowledgements

The authors thank Ginette Dubuc, Shirley and Richard Auprix and Dr. Andrew Sparling for help with llama immunizations and blood processing and Nathalie Gaudette for helpful suggestions during the construction of the llama immune library. We appreciate the work of Dan Jarrell, Yang Shao, and Chris Langley in the production and purification of sdAbs and the pentabody. We are grateful to Denise Boulais and Brian Cass for production and purification of cHCAb and to Suzanne Grothé for assistance with the Biacore analyses. Thanks to Tom Devecseri and Tomoko Hirama for help with the preparation of the figures. We are also grateful to Dr. M. Neuberger for providing the DNA for human IgG1. This work was supported by funding from the NRC Genomics and Health Initiative, Canadian Institutes of Health Research, San Antonio Life Science Institute (10003177) and a start-up fund from Department of Radiology, University of Texas Health Science Center at San Antonio. The ^{64}Cu was provided by Washington University Research Resource in Radionuclide Research (R24CA086307).

References

[1] S. Sebastian, J. Settleman, S.J. Reshkin, A. Azzariti, A. Bellizzi, A. Paradiso, The complexity of targeting EGFR signalling in cancer: from expression to turnover, Biochim. Biophys. Acta 1766 (2006) 120–139.
[2] G. Carpenter, Receptors for epidermal growth factor and other polypeptide mitogens, Annu. Rev. Biochem. 56 (1987) 881–914.
[3] J.D. Sato, T. Kawamoto, A.D. Le, J. Mendelsohn, J. Polikoff, G.H. Sato, Biological effects in vitro of monoclonal antibodies to human epidermal growth factor receptors, Mol. Biol. Med. 1 (1983) 511–529.
[4] M. Jain, S.C. Chauhan, A.P. Singh, G. Venkatraman, D. Colcher, S.K. Batra, Penetratin improves tumor retention of single-chain antibodies: a novel step toward optimization of radioimmunotherapy of solid tumors, Cancer Res. 65 (2005) 7840–7846.
[5] F. Trejtnar, M. Laznicek, Analysis of renal handling of radiopharmaceuticals, Quart. J. Nucl. Med. 46 (2002) 181–194.
[6] A. Goel, D. Colcher, J. Baranowska-Kortylewicz, S. Augustine, B.J. Booth, G. Pavlinkova, et al., Genetically engineered tetravalent single-chain Fv of the pancarcinoma monoclonal antibody CC49: improved biodistribution and potential for therapeutic application, Cancer Res. 60 (2000) 6964–6971.
[7] S. Hu, L. Shively, A. Raubitschek, M. Sherman, L.E. Williams, J.Y. Wong, et al., Minibody: a novel engineered anti-carcinoembryonic antigen antibody fragment (single-chain Fv-CH3) which exhibits rapid, high-level targeting of xenografts, Cancer Res. 56 (1996) 3055–3061.
[8] G.P. Adams, R. Schier, A.M. McCall, H.H. Simmons, E.M. Horak, R.K. Alpaugh, et al., High affinity restricts the localization and tumor penetration of single-chain fv antibody molecules, Cancer Res. 61 (2001) 4750–4755.
[9] A.M. Wu, G.J. Tan, M.A. Sherman, P. Clarke, T. Olafsen, S.J. Forman, et al., Multimerization of a chimeric anti-CD20 single-chain Fv-Fc fusion protein is mediated through variable domain exchange, Protein Eng. 14 (2001) 1025–1033.
[10] V. Kenanova, T. Olafsen, L.E. Williams, N.H. Ruel, J. Longmate, P.J. Yazaki, et al., Radioiodinated versus radiometal-labeled anti-carcinoembryonic antigen single-chain Fv-Fc antibody fragments: optimal pharmacokinetics for therapy, Cancer Res. 67 (2007) 718–726.
[11] R. To, T. Hirama, M. Arbabi-Ghahroudi, R. MacKenzie, P. Wang, P. Xu, et al., Isolation of monomeric human V(H)s by a phage selection, J. Biol. Chem. 280 (2005) 41395–41403.
[12] L. Jespers, O. Schon, K. Famm, G. Winter, Aggregation-resistant domain antibodies selected on phage by heat denaturation, Nat. Biotechnol. 22 (2004) 1161–1165.
[13] C. Hamers-Casterman, T. Atarhouch, S. Muyldermans, G. Robinson, C. Hamers, E.B. Songa, et al., Naturally occurring antibodies devoid of light chains, Nature 363 (1993) 446–448.
[14] A.S. Greenberg, D. Avila, M. Hughes, A. Hughes, E.C. McKinney, M.F. Flajnik, A new antigen receptor gene family that undergoes rearrangement and extensive somatic diversification in sharks, Nature 374 (1995) 168–173.
[15] H. Revets, P. De Baetselier, S. Muyldermans, Nanobodies as novel agents for cancer therapy, Expert Opin. Invest. Drugs 5 (2005) 111–124.
[16] M. Dumoulin, K. Conrath, A. Van Meirhaeghe, F. Meersman, K. Heremans, L.G. Frenken, et al., Single-domain antibody fragments with high conformational stability, Protein Sci. 11 (2002) 500–515.
[17] M. Arbabi Ghahroudi, A. Desmyter, L. Wyns, R. Hamers, S. Muyldermans, Selection and identification of single domain antibody fragments from camel heavy-chain antibodies, FEBS Lett. 414 (1997) 521–526.
[18] S. Li, W. Zheng, R. Kuolee, T. Hirama, M. Henry, S. Makvandi-Nejad, et al., Pentabody-mediated antigen delivery induces antigen-specific mucosal immune response, Mol. Immunol. 46 (2009) 1718–1726.
[19] J. Davies, L. Riechmann, Affinity improvement of single antibody VH domains: residues in all three hypervariable regions affect antigen binding, Immunotechnology 2 (1996) 169–179.
[20] E. De Genst, F. Handelberg, A. Van Meirhaeghe, S. Vynck, R. Loris, L. Wyns, et al., Chemical basis for the affinity maturation of a camel single domain antibody, J. Biol. Chem. 279 (2004) 53593–53601.
[21] V. Cortez-Retamozo, M. Lauwereys, G. Hassanzadeh Gh, M. Gobert, K. Conrath, S. Muyldermans, et al., Efficient tumor targeting by single-domain antibody fragments of camels, Int. J. Cancer 98 (2002) 456–462.
[22] V. Cortez-Retamozo, N. Backmann, P.D. Senter, U. Wernery, P. De Baetselier, S. Muyldermans, et al., Efficient cancer therapy with a nanobody-based conjugate, Cancer Res. 64 (2004) 2853–2857.
[23] Q.F. Miao, X.Y. Liu, B.Y. Shang, Z.G. Ouyang, Y.S. Zhen, An enediyne-energized single-domain antibody-containing fusion protein shows potent antitumor activity, Anticancer Drugs 18 (2007) 127–137.
[24] R.C. Roovers, T. Laeremans, L. Huang, S. De Taeye, A.J. Verkleij, H. Revets, et al., Efficient inhibition of EGFR signaling and of tumour growth by antagonistic anti-EFGR nanobodies, Cancer Immunol. Immunother. 56 (2007) 303–317.
[25] K. Omidfar, M.J. Rasaee, H. Modjtahedi, M. Forouzandeh, M. Taghikhani, N. Golmakani, Production of a novel camel single-domain antibody specific for the type III mutant EGFR, Tumour Biol. 25 (2004) 296–305.
[26] L.O. Gainkam, L. Huang, V. Caveliers, M. Keyaerts, S. Hernot, I. Vaneycken, et al., Comparison of the biodistribution and tumor targeting of Two 99mTc-labeled Anti-EGFR nanobodies in mice, using pinhole SPECT/micro-CT, J. Nucl. Med. 49 (2008) 788–795.
[27] L. Huang, L.O. Gainkam, V. Caveliers, C. Vanhove, M. Keyaerts, P. De Baetselier, et al., SPECT imaging with (99 m)Tc-labeled EGFR-specific nanobody for in vivo monitoring of EGFR expression, Mol. Imaging Biol. 10 (2008) 167–175.
[28] P.M. Brown, M.T. Debanne, S. Grothe, D. Bergsma, M. Caron, C. Kay, et al., The extracellular domain of the epidermal growth factor receptor, Studies on the affinity and stoichiometry of binding, receptor dimerization and a binding-domain mutant, Eur. J. Biochem. 225 (1994) 223–233.
[29] M.J. Campa, C.T. Kuan, M.D. O'Connor-McCourt, D.D. Bigner, E.F. Patz Jr., Design of a novel small peptide targeted against a tumor-specific receptor, Biochem. Biophys. Res. Commun. 275 (2000) 631–636.
[30] J. Tanha, A. Muruganandam, D. Stanimirovic, Phage display technology for identifying specific antigens on brain endothelial cells, Methods Mol. Med. 89 (2003) 435–449.
[31] E. Stone, T. Hirama, J. Tanha, H. Tong-Sevinc, S. Li, C.R. MacKenzie, et al., The assembly of single domain antibodies into bispecific decavalent molecules, J. Immunol. Methods 318 (2007) 88–94.
[32] J. Zhang, Q. Li, T.D. Nguyen, T.L. Tremblay, E. Stone, R. To, et al., A pentavalent single-domain antibody approach to tumor antigen discovery and the development of novel proteomics reagents, J. Mol. Biol. 341 (2004) 161–169.
[33] Y. Durocher, S. Perret, A. Kamen, High-level and high-throughput recombinant protein production by transient transfection of suspension-growing human 293-EBNA1 cells, Nucleic Acids Res. 30 (2002) E9.

[34] J. Zhang, X. Liu, A. Bell, R. To, T.N. Baral, A. Azizi, et al., Transient expression and purification of chimeric heavy chain antibodies, Protein Expression Purif. 65 (2009) 77–82.
[35] P.L. Pham, S. Perret, B. Cass, E. Carpentier, G. St-Laurent, L. Bisson, et al., Transient gene expression in HEK293 cells: peptone addition posttransfection improves recombinant protein synthesis, Biotechnol. Bioeng. 90 (2005) 332–344.
[36] S.C. Gill, P.H. Von Hippel, Calculation of protein extinction coefficients from amino acid sequence data, Anal. Biochem. 182 (1989) 319–326.
[37] G. Sakaue, T. Hiroi, Y. Nakagawa, K. Someya, K. Iwatani, Y. Sawa, et al., HIV mucosal vaccine: nasal immunization with gp160-encapsulated hemagglutinating virus of Japan-liposome induces antigen-specific CTLs and neutralizing antibody responses, J. Immunol. 170 (2003) 495–502.
[38] H. Ling, A. Boodhoo, B. Hazes, M.D. Cummings, G.D. Armstrong, J.L. Brunton, et al., Structure of the shiga-like toxin I B-pentamer complexed with an analogue of its receptor Gb3, Biochemistry 37 (1998) 1777–1788.
[39] F.R. Luo, Z. Yang, H. Dong, A. Camuso, K. McGlinchey, K. Fager, et al., Correlation of pharmacokinetics with the antitumor activity of Cetuximab in nude mice bearing the GEO human colon carcinoma xenograft, Cancer Chemother. Pharmacol. 56 (2005) 455–464.
[40] C.P. Graff, K.D. Wittrup, Theoretical analysis of antibody targeting of tumor spheroids: importance of dosage for penetration, and affinity for retention, Cancer Res. 63 (2003) 1288–1296.
[41] X. Xu, P. Clarke, G. Szalai, J.E. Shively, L.E. Williams, Y. Shyr, et al., Targeting and therapy of carcinoembryonic antigen-expressing tumors in transgenic mice with an antibody-interleukin 2 fusion protein, Cancer Res. 60 (2000) 4475–4484.
[42] D.C. Slavin-Chiorini, S.V. Kashmiri, J. Schlom, B. Calvo, L.M. Shu, M.E. Schott, et al., Biological properties of chimeric domain-deleted anticarcinoma immunoglobulins, Cancer Res. 55 (1995) 5957s–5967s.
[43] L.A. Khawli, B. Biela, P. Hu, A.L. Epstein, Comparison of recombinant derivatives of chimeric TNT-3 antibody for the radioimaging of solid tumors, Hybrid Hybridom. 22 (2003) 1–9.
[44] F. Buchegger, C.M. Haskell, M. Schreyer, B.R. Scazziga, S. Randin, S. Carrel, et al., Radiolabeled fragments of monoclonal antibodies against carcinoembryonic antigen for localization of human colon carcinoma grafted into nude mice, J. Exp. Med. 158 (1983) 413–427.
[45] L. Jespers, O. Schon, L.C. James, D. Veprintsev, G. Winter, Crystal structure of HEL4, a soluble, refoldable human V(H) single domain with a germ-line scaffold, J. Mol. Biol. 337 (2004) 893–903.